JOURNAL OF AGRICULTURAL AND FOOD CHEMISTRY
ARTICLE

J. Agric. Food Chem. 2009, 57, 4913–4923 4913
DOI:10.1021/jf900286x

# Differences in Pig Muscle Proteome According to HAL Genotype: Implications for Meat Quality Defects

Elisabeth Laville,*,† Thierry Sayd,† Claudia Terlouw,§ Sylvie Blinet,†
Jeremy Pinguet,# Martine Fillaut,⊥ Jérome Glénisson,∥ and Pierre Chérel∥

†INRA, UR370, Qualité des Produits Animaux and §INRA, UR1213 Unité de Recherches sur les Herbivores and #INRA, Plate-Forme d'Exploration du Métabolisme, pôle Protéome, Theix, 63122 Saint-Genès-Champanelle, France, ⊥INRA, UMR1079, Unité Mixte de Recherches Systèmes d'Elevage Nutrition Animale et Humaine, 35590 Saint-Gilles, France, and ∥France Hybrides, 45808 St Jean de Braye, France

Bidimensional electrophoresis was used to compare sarcoplasmic protein profiles of early post-mortem pig semimembranosus muscles, sampled from pigs of different HAL genotypes (RYR1 mutation 1841T/C): 6 NN, 6 Nn, 6 nn. ANOVA showed that 55 (18%) of the total of 300 matched protein spots were influenced by genotype, and hierarchical clustering analysis identified 31 (10% of the matched proteins) additional proteins coregulated with these proteins. Fold-changes of differentially expressed proteins were between 1.3 and 21.8. Peptide mass fingerprinting identification of 78 of these 86 proteins indicates that faster pH decline of nn pigs was not explained by higher abundance of glycolytic enzymes. Results indicate further that nn muscles contained fewer proteins of the oxidative metabolic pathway, fewer antioxidants, and more protein fragments. Lower abundance of small heat shock proteins and myofibrillar proteins in nn muscles may at least partly be explained by the effect of pH on their extractability. Possible consequences of lower levels of antioxidants and repair capacities, increased protein fragmentation, and lower extractability of certain proteins in nn muscles on meat quality are discussed.

**KEYWORDS: 2-DE gels; pig muscle; hierarchical clustering analysis; malignant hyperthermia; meat quality; energetic metabolism; heat shock proteins; antioxidant proteins**

## INTRODUCTION

In some porcine populations, malignant hyperthermia (MH) is a heritable trait resulting from a mutation on the ryanodine receptor (RYR1) gene known as halothane (Hal locus) (*1*). This gene encodes a calcium release channel protein of the sarcoplasmic reticulum, and the identified mutation is responsible for sudden increases in calcium levels in the cytoplasm during challenges (*2*). The MH syndrome may be induced by anesthetics such as halothane and by stress. Such uncontrolled sarcoplasmic $Ca^{2+}$ release via the ryanodine receptor activates actomyosin filaments leading to muscle contractions and triggers glycogenolysis, resulting in anoxia, muscle acidosis, and heat production. Stress occurs often during the preslaughter period due to mixing, transport, and handling (*3*). Consequently, the mutation may be a cause of mortality during transport or, when occurring just before slaughter, of reduced quality of the meat, which becomes pale, soft, and exsudative (PSE) (*4*). In halothane-induced hyperthermia, the RYR1 mutation is considered to be fully recessive. However, there is some evidence that calcium homeostasis is also disturbed in heterozygous pigs (*5*). Most studies report that heterozygous carriers have intermediate meat quality traits compared to homozygous carriers and noncarriers (*6*, *7*). The reduced meat quality is related to post-mortem muscle metabolism characterized by an increased rate of pH decline associated with an increase in muscle temperature. The combination of low pH at high temperature increases protein denaturation, which is believed to be partly responsible for the development of PSE meat (*8*, *9*).

Identification of causative mutation allowed a full control of RYR1 genotype in pig breeding, with elimination of any mutation carriers in dam line populations, to prevent production of nn genotype animals in production. Despite this selection, meat with poor water-holding capacity and light color is still observed in HAL NN genotype animals (*10*). To potentially detect which live animals are susceptible to develop PSE meat, which would be essential for further breeding improvement, we would benefit from being able to recognize the characteristics of muscles from pigs carrying the RYR1 mutation, as a genetic model of a common meat quality defect. Proteins play an important role in the development of PSE defect during post-mortem stages (*11*). There is, however, relatively little information on the effect of RYR1 mutation on protein levels. Particularly, the effect of leakage of calcium from the channel on proteins involved in cellular metabolism needs to be elucidated. Therefore, in the present study, using bidimensional gel electrophoresis (2-DE), we compared muscle proteome profiles of pigs that were

*Author to whom correspondence should be addressed [telephone +33 (0)4 73 62 48 34; fax +33 (0)4 73 62 42 68; e-mail elaville@clermont.inra.fr].

 Published on Web 05/18/2009 

heterozygous or homozygous carriers or noncarriers of the RYR1 mutation to identify protein mechanisms underlying meat PSE defects. We have chosen to focus on the study of the soluble fraction, which contains mainly sarcoplasmic proteins and represents only 30% of the total proteome of the cell but which includes most of the proteins involved in energy metabolism regulation and signal transduction pathways. The soluble fraction excludes to a large extent myofibrillar proteins, membranes, and connective tissue but increases the gel resolution of the studied fraction and thus the number of proteins that can be quantified.

## MATERIAL AND METHODS

**Animals and Carcass Sampling.** Muscles were sampled from pigs produced as an F2 intercross obtained from two production sire lines: FH016 (Pietrain type, France Hybrides SA, St Jean de Braye, France) and FH019 (synthetic line, from Duroc, Hampshire, and Large White founders, France Hybrides SA). Pigs of the F2 population ($N = 1000$) were tested for RYR1 polymorphism (*12*) and 18 of them, with the same sire, were selected to be compared: 6 homozygous normal (NN), 6 heterozygous (Nn), and 6 homozygous for the mutation (nn). Pigs were slaughtered at an average carcass weight of 92.7 kg under commercial conditions. Five-gram samples were collected from the dorsosuperficial region of semimembranosus (SM) muscle 20 min after stunning. Samples were immediately snap frozen in liquid nitrogen and subsequently stored at −80 °C for proteomic analysis. Forty-five minutes after stunning, 1 g samples were collected of the longissimus lomborum (LL) muscle at the levels of the last rib and immediately ground in 18 mL of a 5 mM iodoactetate solution to measure the pH of the homogenate ($pH_{45(LL)}$) with a glass electrode (Mettler Toledo, Switzerland) connected to a portable pH-meter (Schött-Geräte, Germany). One hour post-mortem, half-carcasses were introduced in the cold room (12 °C) for 4 h and subsequently stored at 3 °C. Twenty-four hours post-mortem the pH was recorded directly on the carcass in the loin ($pH_{u(LL)}$) and in the SM ($pH_{u(SM)}$). Thirty-six hours post-mortem loins were kept for 30 min at −10 °C to make them rigid to allow slicing with an automated industrial cutter, irrespective of anatomical rib boundaries. Two slices of 4 cm width (326 ± 65 g) including the 11th and 12th ribs were collected for each loin. About 10 g of one slice was used for chemical analyses. The remaining part was used for color measurement and for raw meat shear force determination. The second slice was weighed and kept at 4 °C in a closed plastic bag to measure drip loss 48 h later, expressed as percent of initial weight. The slice was subsequently used to determine cooked meat shear force.

**Chemical and Physical Characterization of Meat.** Characterization of meat was performed on the 1000 pigs of the F2 population. Ultimate pH was assessed on both the SM and LL muscle. The other chemical and physical indicators of meat quality were assessed on the LL muscle. The following measurements, previously described (*13*), were performed on raw meat: $pH_{45(LL)}$, $pH_{u(LL)}$, $pH_{u(SM)}$, drip loss (DL) and cooking loss (CL), lightness ($L^*$), intramuscular fat (IMF), and glycolytic potential (GP). Warner−Bratzler shear force (WBSF) was assessed on both raw and cooked meat (*13*).

**Soluble Protein Extraction and Two-Dimensional Gel Electrophoresis.** Proteomic analysis was performed on the samples of SM muscles of the 18 pigs selected according to RYR1 polymorphism. The 2-DE gels were carried out on 1 g of thawed muscle as previously described (*14*). Briefly, muscle was homogenized, using a glass bead agitator MM2 (Retsch, Haan, Germany), in 40 mM Tris (pH 8), 2 mM EDTA, and a protease inhibitor cocktail (Sigma) at 4 °C, at the ratio of 1:4 (w/v). The homogenate was centrifuged at 4 °C for 10 min at 10000*g*. Supernatant, referred to as the soluble extract, was stored at −80 °C until further assaying. Protein concentration was determined according to the Bradford assay (Bio-Rad, Hercules, CA). Nine hundred micrograms of sarcoplamic proteins was included in a buffer containing 7 M urea, 2 M thiourea, 2% (w/v) CHAPS, 0.4% (v/v) carrier ampholyte, and bromophenol blue. Samples were loaded onto immobilized pH-gradient strips (pH 5−8, 17 cm, Bio-Rad), and isoelectric focusing was performed using a Protean IEF cell system (Bio-Rad). Gels were passively rehydrated for 16 h. Rapid voltage ramping was subsequently applied to reach a total of 85 kVh. In the second dimension, proteins were resolved on 12% SDS-PAGE gels using Protean II XL system (Bio-Rad). Gels were Coomassie Blue (colloidal blue) stained as previously described (*15*). Two gels were produced per sample.

**Gel Visualization, Image Acquisition, and Statistical Analysis.** Gel images were acquired using a GS-800 imaging densitometer (Bio-Rad) and analyzed using the 2-DE image analysis software PDQuest (Bio-Rad). Image analysis was performed as previously described (*14*). Normalized protein abundance of detected spots was calculated as spot intensity for an individual spot divided by spot intensity for all valid spots. The intensity-dependent distribution of spots was assessed according to the technique of Meunier et al. and found to be normal (*16*). Statistical analyses were performed using SAS software version 8 (SAS Institute, Inc., Cary, NC). The ANOVA procedure was used to test significance ($p < 0.05$) of the fixed effect of genotype (NN, Nn, nn) on meat characteristics (IMF, GP, pHu, $pH_{45}$, $L^*$, DL, CL, WBSF of raw and cooked meat) and on log-ratio values of normalized intensities of valid spots. When different spot intensities were found between genotypes, relevant phenotypic characteristics (Bradford and pH values) were introduced as covariate in the ANOVA to study possible relationships while correcting for genotype effects. Principal component analysis was carried out on relevant meat variables and correlated spots to produce plots illustrating relationships between meat characteristics and protein content. One-sided binomial analysis was used to assess whether the proportion of spots influenced by genotype was greater than the proportion expected by chance (5%). When significant effects were found, Bonferroni comparison tests were used to identify differences between pairs of groups at the 5% significance level. In addition, a hierarchical clustering analysis (HCA) using PermutMatrix software (http://www.lirmm.fr/~caraux/PermutMatrix/; LIRMM, Montpellier, France) was performed after a log-ratio transformation to explore and visualize which spots have similar expression profiles (*17*). Ward's dissimilarity aggregation procedure based on Pearson distances was used as recommended (*18*). The one-way HCA was applied to matched spots to construct a dendrogram of coregulated proteins.

**In-Gel Digestion and Proteins Identification by Mass Spectrometry.** Coomassie-stained spots of interest were manually excised using pipet tips. The spots where then destained with 100 μL of 25 mM $NH_4HCO_3$ and 5% v/v acetonitrile for 30 min, followed by 100 μL of 25 mM $NH_4HCO_3$ and 50% v/v acetonitrile and then dehydrated in acetonitrile. Gel spots were completely dried using a Speed Vac before trypsin digestion at 37 °C over 5 h with 15 μL of trypsin (10 ng/μL; V5111, Promega, Madison, WI) in 25 mM $NH_4HCO_3$. Peptide extraction was optimized by adding 8 μL of acetronitile, followed by 5 min of sonication. For matrix-assisted laser desorption/ionization−time-of-flight (MALDI-TOF) mass spectrometry analysis, 1 μL of supernatant was loaded directly onto the MALDI target. The matrix solution (5 mg/mL of α-cyano-4-hydroxycinnamic acid in 50% acetonitrile, 0.1% trifluoroacetic acid) was immediately added and allowed to dry at room temperature.

Peptide mass fingerprint (PMF) of trypsin-digested spots was determined in positive-ion reflector mode using a Voyager DE Pro MALDI-TOF-MS (PerSeptive Biosystems, Framingham, MA). External calibration was performed with a standard peptide solution (Peptide Mix 4, Proteomix, LaserBio Laboratories, Sophia-Antipolis, France). A total of 1000 shots from the nitrogen laser operating at 337 nm were accumulated for each spot. The spectra were internally calibrated using trypsin autolysis peaks followed by baseline correction, deisotoping, and noise filtration. The resulting peak lists were generated by DataExplorer 4.0 software (Applied Biosystems). PMFs were compared to *Mammalia* nrNCBI (12/2008, 1 2219 208 seq) protein sequence databases (http://www.ncbi.nlm.nih.gov/Database/) using MASCOT 2.2 software [http://www.matrixscience.com (last accessed January 2009)]. The initial search parameters allowed a single trypsin missed cleavage, partial carbamidomethylation of cysteine, partial oxidation of methionine, and mass deviation lower than 25 ppm. We required at least five matched peptides per protein for identification and used MASCOT probabilistic scores, accuracy of the experimental-to-theoretical p*I*, and molecular weight (MW).

**Monodimensional Gel Electrophoresis and Western Blotting.** Monodimensional gel electrophoresis (1-DE) was carried out on the soluble fraction. Samples were separated on the 12% SDS−polyacrylamide. The 1-DE and 2-DE gels were transferred to polyvinylidene difluoride membranes using a trans-blot apparatus (GE Healthcare, Saclay, France).

Membranes were blocked with 5% w/v skim milk in TBS with 0.05% v/v Tween 20 and incubated overnight in appropriate dilutions of the following polyclonal antibodies: rabbit anti-heat-shock cognate 71, rabbit anti-heat-shock protein 27, and rabbit anti-α crystallin β chain (Stressgen, Victoria, Canada). After extensive washing, membranes were incubated with 1:10000 anti-rabbit IgG horseradisch peroxidase (GE Healthcare) for 1 h and washed before detection by ECL Plus chemiluminescence detection reagent (GE Healthcare). The intensity of bands revealed with ECL Plus chemiluminescence was quantified with Quantity one 1-D analysis software (Bio-Rad).

## RESULTS

**Chemical and Physical Characterization of Meat.** Results are presented in **Table 1**. The protein concentrations of sarcoplasmic extract determined according to the Bradford assay were not different between genotypes. The nn genotype had lower $pH_{45(LL)}$ values and lower WBSF of raw meat. Genotypes did not differ in $pH_{u(LL)}$ and $pH_{u(SM)}$ values or in WBSF of cooked meat, GP, $L^*$, IMF, DL, and CL.

**Proteomic Analysis.** On 2-DE gels, 55 of the 300 matched spots showed a significant differential abundance between the 3 groups (entries in bold in **Tables 2−6**). Of these proteins, 29 were more abundant in the NN compared to the Nn and nn genotypes. Fifty-one of the 55 spots were successfully identified using peptide mass fingerprinting. Thirty-nine of the 55 differentially expressed spots were assigned by HCA to four clusters of proteins, along with 31 other coregulated proteins (**Figure 1**). These clusters clearly identified the largest part of proteome variation associated with genotype. Clusters 1−3 contained proteins up-regulated in the NN genotype. Levels of these proteins were intermediate in the Nn genotype. Cluster 4 corresponded to proteins over-represented in the nn genotype relative to the NN and Nn genotypes. Twenty-seven of the additional 31 spots in these four clusters were identified using peptide mass fingerprinting (**Tables 2−6**). **Figure 2** shows a representative gel of soluble muscle proteins; positions of the spots identified by mass spectrometry are encircled.

*(i) Cluster 1* (**Table 2**) contains four proteins of the aldehyde dehydrogenase family involved in cell detoxification; four cytoskeletal proteins; two isoforms of the mitochondrial ATP synthase; lactate dehydrogenase, an enzyme of the anaerobic glycolytic pathway; a subunit of a proteolytic enzyme; and copine, which is a calcium-dependent protein involved in membrane trafficking.

*(ii) Cluster 2* (**Table 3**) contains several chaperone proteins: isoforms of heat-shock protein 27 (Hsp27) and α β-crystalline

**Table 1.** Mean and Standard Deviation of Meat Characteristics Measured on the Longissimus Dorsi (LD) Muscle and Group Effect (NN, Homozygous Normal; Nn, Heterozygous; nn, Homozygous Mutant)

| meat characteristic[a] | population $N = 1000$ | NN group $N = 6$ | Nn group $N = 6$ | nn group $N = 6$ | $Pr > F$[c] |
|---|---|---|---|---|---|
| protein concentration | | 86.5 ± 3.4 | 89.48 ± 9.5 | 82.47 ± 8.5 | 0.269 |
| WBSF raw | 35.9 ± 6.5 | **33.86 ± 7.4** | 27.06 ± 5.8 | 25.3 ± 4 | 0.0435 |
| WBSF cooked | 34 ± 5.4 | 34.23 ± 4.4 | 32.04 ± 2.5 | 36.9 ± 5.6 | 0.1464 |
| IMF | 2.2 ± 0.7 | 2.5 ± 0.5 | 2.7 ± 0.8 | 2.7 ± 0.6 | 0.8089 |
| GP | 162.4 ± 25.1 | 187.8 ± 23.6 | 164.5 ± 35.2 | 173.6 ± 20.3 | 0.3300 |
| $pH_{u\ (SM)}$[b] | 5.7 ± 0.01 | 5.7 ± 0.1 | 5.6 ± 0.1 | 5.6 ± 0.1 | 0.9311 |
| $pH_u$ | 5.7 ± 0.2 | 5.5 ± 0.1 | 5.5 ± 0.1 | 5.5 ± 0.04 | 0.5167 |
| $pH_{45}$ | 6.5 ± 0.2 | **6.5 ± 0.1** | **6.2 ± 0.1** | **5.8 ± 0.2** | <0.0001 |
| $L^*$ | 49.6 ± 3.3 | 52.5 ± 3.4 | 53.6 ± 2.8 | 51.3 ± 2.4 | 0.2491 |
| DL | 1.6 ± 1 | 2.2 ± 0.7 | 3.1 ± 1.2 | 4.1 ± 1.7 | 0.0604 |
| CL | 25.9 ± 4.6 | 27.7 ± 3.3 | 28.4 ± 2.9 | 28.6 ± 1.8 | 0.8213 |

[a] WBSF, Warner−Bratzler shear force; IMF, intramuscular fat; GP, glycolytic potential; $pH_u$, ultimate pH; $pH_{45}$, pH at 45 min; $L^*$, lightness; DL, drip loss; CL, cooking loss. [b] Measure of ultimate pH was also performed on the semimembranosus muscle. [c] $p < 0.05$: differences are significant. Within a row differences between groups are indicated in bold.

**Table 2.** Pig Semimembranosus Muscle Proteins Evidenced in Cluster 1 according to HCA

| | | | | | | $M_w$ (kDa)/p$I$[e] | | relative abundance[f] | | | |
|---|---|---|---|---|---|---|---|---|---|---|---|
| spot | protein name[a] | accession no.[a] | mowse score[b] | sequence coverage[c] | MP[d] | theor | obsd | NN vs nn | NN vs Nn | Nn vs nn | spot $p$ value[g] |
| **2504** | mitochondrial aldehyde dehydrogenase 2 | gil113205888 | 120 | 24 | 13 | 53.4/6.01 | 56.0/6.04 | 1.4*[h] | 1.4 | 1.0 | 0.023 |
| **1618** | mitochondrial aldehyde dehydrogenase 2 | gil113205888 | 105 | 40 | 17 | 56.9/6.4 | 56.9/5.87 | 1.7* | 1.8 | −1.0 | 0.019 |
| 1509 | γ- aminobutaldehyde dehydrogenase | gil1049219 | 74 | 16 | 8 | 53.4/6.01 | 53.4/5.8 | | | | NS |
| 3520 | *S*-adenosylhomocysteinase | gil58801555 | 126 | 32 | 15 | 47.6/5.88 | 44.7/6.17 | | | | NS |
| 0501 | mitochondrial ATP synthase, β subunit | gil89574051 | 151 | 51 | 20 | 47/4.99 | 51.6/4.82 | | | | NS |
| 0502 | mitochondrial ATP synthase, β subunit | gil89574051 | 123 | 45 | 15 | 47/4.99 | 51.9/4.92 | | | | NS |
| 1305 | L-lactate dehydrogenase B | gil164518958 | 77 | 33 | 10 | 36.5/5.57 | 36.7/5.67 | | | | NS |
| **0103** | myosin light chain 1f | gil117660874 | 92 | 45 | 8 | 20.9/4.90 | 26.3/4.86 | 1.9* | 1.5 | 1.2 | 0.030 |
| 0112 | myosin light chain 1f | gil117660874 | 75 | 51 | 9 | 20.9/4.9 | 25.9/5.0 | | | | NS |
| 0109 | myosin light chain 1f | gil117660874 | 155 | 67 | 16 | 20.9/4.9 | 26.5/4.91 | | | | NS |
| **0630** | tubulin, α 4a | gil194043859 | 207 | 58 | 24 | 49.8/4.95 | 59.1/4.97 | 5.1* | 1.3 | 3.8* | 0.0001 |
| **1723** | copine-1, isoform 8 | gil184185560 | 83 | 16 | 9 | 58.8/5.43 | 65.6/5.57 | 3.1* | 1.7 | 1.8* | 0.011 |
| 4101 | proteasome subunit β type-2 | gil1709762 | 86 | 42 | 9 | 22.8/6.51 | 26.4/6.41 | | | | NS |
| **2506** | albumin, **fgm**[i] | gil833798 | 96 | 38 | 21 | 69.3/9.92 | 53.9/6.08 | 2.2* | 2.0* | 1.1 | 0.006 |

[a] Protein name and accession numbers were derived from NCBI database. [b] The MASCOT baseline significant score is 66. [c] Percent of coverage of the entire amino acid sequence. [d] Number of matched peptides in the database search. [e] MW and p$I$, theoretical (recorded in NCBI database) and observed (calculated from the spot position on the gel). [f] Relative abundance: greatest average quantity/lowest average quantity. A minus sign in comparisons of NN and nn, NN and Nn, and Nn and nn indicates that the relative abundance of the protein is higher in NN (homozygous normal), Nn (heterozygous), and nn (homozygous mutant) groups, respectively. [g] $p$ value from the ANOVA analysis of genotype effect (spot numbers in bold are significantly influenced by genotype). [h] Asterisk indicates difference according to the Bonferroni pairwise comparison between genotypes at the 5% significance level. [i] **fgm**, protein fragment.

**Table 3.** Pig Semimembranosus Muscle Proteins Evidenced in Cluster 2 according to HCA

| spot | protein name [a] | accession no. [a] | mowse score [b] | sequence coverage [c] | MP [d] | $M_w$ (kDa)/p*I* theor [e] | $M_w$ (kDa)/p*I* obsd [e] | relative abundance [f] NN vs nn | relative abundance [f] NN vs Nn | relative abundance [f] Nn vs nn | spot *p* value [g] |
|---|---|---|---|---|---|---|---|---|---|---|---|
| 4102 | Hsp27 | gil55668280 | 83 | 37 | 9 | 22.9/6.23 | 28.9/6.42 | | | | NS |
| 2103 | Hsp27 | gil55668280 | 84 | 35 | 8 | 22.9/6.23 | 28.6/6.00 | | | | NS |
| **1101** [i] | Hsp27 | gil85542053 | 71 | 38 | 6 | 22.3/5.98 | 28.7/5.61 | 4.2*[h] | 1.7 | 2.4 | 0.025 |
| 5016 | α crystallin B chain | gil169882027 | 120 | 61 | 11 | 20.1/6.76 | 22.1/5.61 | | | | NS |
| 6022 | α crystallin B chain | gil75063982 | 101 | 45 | 11 | 20.1/6.76 | 23.8/6.76 | | | | NS |
| 7008 | α crystallin B chain | gil169882027 | 133 | 61 | 13 | 20.1/6.76 | 23.9/6.98 | | | | NS |
| 5019 [j] | α crystallin B chain | | | | | | 24.3/6.6 | | | | NS |
| **0005** | myosin regulatory light chain 2 | gil117660856 | 81 | 41 | 8 | 18.9/4.82 | 19.9/4.9 | 21.8* | 4.0 | 5.5 | 0.023 |
| 2410 | succinyl-CoA ligase, β-chain, mitochondrial | gil21263966 | 75 | 19 | 8 | 46.2/6.08 | 43.3/6.09 | | | | NS |
| **2402** | dihydrolipoamide *S*-succinyltransferase | gil47523848 | 91 | 18 | 7 | 48.9/9.0 | 43.2/5.96 | 2.1 | 1.1 | 2* | 0.018 |
| 0203 | proteasome subunit α type 3 | gil194034199 | 107 | 44 | 13 | 27.6/5.29 | 29.8/5.28 | | | | NS |
| **2806** | thimet oligopeptidase | gil1871406 | 82 | 29 | 25 | 78/5.82 | 82.2/6.15 | 2.7* | 1.2 | 2.2 | 0.026 |

[a] Protein name and accession numbers were derived from NCBI database. [b] The MASCOT baseline significant score is 66. [c] Percent of coverage of the entire amino acid sequence. [d] Number of matched peptides in the database search. [e] MW and p*I*, theoretical (recorded in NCBI database) and observed (calculated from the spot position on the gel). [f] Relative abundance: greatest average quantity/lowest average quantity. A minus sign in comparisons of NN and nn, NN and Nn, and Nn and nn indicates that the relative abundance of the protein is higher in nNN (homozygous normal), Nn (heterozygous), and nn (homozygous mutant) groups, respectively. [g] *p* value from the ANOVA analysis of genotype effect (spot numbers in bold are significantly influenced by genotype). [h] Asterisk indicates difference according to the Bonferroni pairwise comparison between genotypes at the 5% significance level. [i] MS spectrum analyzed for post-translational modifications detected two probable phosphorylation sites at two positions corresponding to the serine residues (positions 15 and 82) on peptidic masses 1071.44 (**13**−**20 .SPSWDPFR)** and 1698.78 (**82**−**96 .QLSSGVSEIQQTADR**). [j] This α β-crystallin spot was identified by 2-DE Western blot.

**Table 4.** Pig Semimembranosus Muscle Proteins Evidenced in Cluster 3 according to HCA

| spot | protein name [a] | accession no. [a] | mowse score [b] | sequence coverage [c] | MP [d] | $M_w$ (kDa)/p*I* theor [e] | $M_w$ (kDa)/p*I* obsd [e] | relative abundance [f] NN vs nn | relative abundance [f] NN vs Nn | relative abundance [f] Nn vs nn | spot *p* value [g] |
|---|---|---|---|---|---|---|---|---|---|---|---|
| **0812** | heat shock cognate 71 kDa protein | gil146324912 | 161 | 35 | 20 | 70.8/5.37 | 73.4/5.33 | 1.3*[i] | 1.2 | 1.1 | 0.029 |
| 1702 | heat shock cognate 71 kDa protein | gil123647 | 133 | 36 | 18 | 70.7/5.24 | 72.3/5.4 | | | | NS |
| 5704 | Hsc70/Hsp90-organizing protein | gil73983760 | 79 | 28 | 19 | 62.5/6.35 | 69.9/6.57 | | | | NS |
| 5718 | T-complex protein, similar to CCT3 protein | gil194036006 | 74 | 17 | 10 | 59.2/7.1 | 70.3/6.61 | | | | NS |
| **1715** | T-complex protein | gil194378060 | 71 | 19 | 10 | 56.6/5.66 | 63.7/5.74 | 2.2* | 1.2 | 1.9 | 0.021 |
| 8023 | actin-modulating protein, cofilin-2 | gil171905897 | 80 | 42 | 8 | 18.7/7.66 | 21.0/7.7 | | | | NS |
| 0124 | translationally controlled tumor protein | gil4507669 | 80 | 52 | 12 | 19.5/4.84 | 26.2/4.7 | | | | NS |
| **0010** | myosin regulatory light chain 2 | gil117660856 | 81 | 46 | 10 | 18.9/4.82 | 19.9/4.75 | 4.7* | 2.3 | 2.0 | 0.004 |
| **0011** | myosin regulatory light chain 2 | gil117660856 | 69 | 66 | 9 | 18.9/4.82 | 19.9/4.79 | 10.6* | 3.4 | 3.1* | 0.001 |
| **0403** | actin, α-1 | gil20664363 | 125 | 47 | 17 | 41.2/5.46 | 42.0/5.23 | 2.3* | 1.2 | 1.9* | 0.0001 |
| **0406** | actin, α-1 | gil20664363 | 133 | 52 | 17 | 41.2/5.46 | 42.5/5.31 | 3.3* | 1.4 | 2.4* | 0.003 |
| 0505 | cAMP-dependent protein kinase type I-α regulatory subunit 3 | gil73965294 | 93 | 32 | 11 | 42.5/5.42 | 49.7/5.33 | | | | NS |
| **0504** | cAMP-dependent protein kinase type I-α regulatory subunit | gil152032553 | 102 | 42 | 14 | 42.9/5.27 | 50.3/5.23 | 5.2* | 1.9 | 2.7 | 0.012 |
| 3522 | aldehyde dehydrogenase family (antiquitin-1) | gil109078417 | 82 | 24 | 11 | 55.3/6.49 | 56.1/6.16 | | | | NS |

[a] Protein name and accession numbers were derived from NCBI database. [b] The MASCOT baseline significant score is 66. [c] Percent of coverage of the entire amino acid sequence. [d] Number of matched peptides in the database search. [e] MW and p*I*, theoretical (recorded in NCBI database) and observed (calculated from the spot position on the gel). [f] Relative abundance: greatest average quantity/lowest average quantity. A minus sign in comparisons of NN and nn, NN and Nn, and Nn and nn indicates that the relative abundance of the protein is higher in NN (homozygous normal), Nn (heterozygous), and nn (homozygous mutant) groups, respectively. [g] *p* value from the ANOVA analysis of genotype effect (spot numbers in bold are significantly influenced by genotype). [i] Asterisk indicates difference according to the Bonferroni pairwise comparison between genotypes at the 5% significance level.

(αβ-C). Another spot was identified as a myosin regulatory light chain, two spots as mitochondrial proteins of tricarboxylic acid cycle, and two others as proteolytic enzymes.

*(iii) Cluster 3* (**Table 4**) was very similar to cluster 2, containing various chaperone proteins involved in protein refolding, assembly, and polymerization. It further contained four structural proteins, the antiquitin protein, involved in cell detoxification, and two isoforms of cAMP-dependent protein kinase (AMPK), which contribute to ATP generation by activating glycolytic enzymes.

*(iv) Cluster 4* corresponded to spots more abundant in the nn genotype (**Table 5**). Most of them were protein fragments of the most abundant glycolytic enzymes. These fragments migrated at a lower molecular weight than their theoretical mass value and cue peptides identified by mass spectrometry, indicating that the spots corresponded to N or C termini of the protein. Other spots of cluster 4 were proteins involved in glycolysis, cell protection, and protein synthesis. One spot was identified as annexin IV, a $Ca^{2+}$-dependent regulative protein involved in membrane organization and ion channel modulation.

*(v) Proteins more abundant in the NN genotype and not included in one of the selected clusters* (**Table 6**) included four proteins involved in cell detoxification, 3 in the dynamic assemblage of structural proteins, and four in energy metabolism. The remaining spot is an isoform of the myosin regulatory light chain 2.

*(vi) Proteins more abundant in the nn genotype and not included in cluster 4* (**Table 6**) include myoglobin, DJ-1 protein, an indicator of oxidative stress, and the iron carrier transferrin.

*(vii) Electrophoretic Variants*. Some of the identified spots were electrophoretic variants or isoforms probably corresponding

**Table 5.** Pig Semimembranosus Muscle Proteins Evidenced in Cluster 4 according to HCA

| | | | | | | $M_w$ (kDa)/p*I* | | relative abundance [f] | | | |
|---|---|---|---|---|---|---|---|---|---|---|---|
| spot | protein name [a] | accession no. [a] | mowse score[b] | sequence coverage[c] | MP [d] | theor[e] | obsd[e] | NN vs nn | N vs Nn | Nn vs nn | spot *p* value [g] |
| **6208** | creatine kinase, muscle **fgm**[j] | gil194018722 | 88 | 22 | 9 | 43.0/6.61 | 32.8/6.77 | −2.5*[i] | −1.8 | −1.4* | 0.0001 |
| **4106** | creatine kinase, muscle **fgm** | gil194018722 | 99 | 30 | 13 | 43.0/6.61 | 28.5/6.52 | −2.3* | −1.8 | −1.3* | 0.0001 |
| **5210** | creatine kinase, muscle **fgm** | gil194018722 | 88 | 28 | 13 | 43.0/6.61 | 31.0/6.7 | −1.6* | −1.0 | −1.6* | 0.002 |
| **6206** | creatine kinase, muscle **fgm** | gil194018722 | 135 | 35 | 16 | 43.0/6.61 | 33.4/6.76 | −2.1* | −1.2 | −1.7* | 0.001 |
| **5326** | creatine kinase, muscle **fgm** | gil194018722 | 118 | 41 | 15 | 43.0/6.61 | 38.0/6.56 | −2.3* | −2.2 | −1.0 | 0.003 |
| **6308** | creatine kinase, muscle **fgm** | gil125305 | 90 | 33 | 13 | 43.0/6.77 | 36/6.81 | −1.7* | −2.2 | 1.3 | 0.028 |
| **5324** | creatine kinase, muscle **fgm** | gil194018722 | 106 | 33 | 14 | 43.0/6.61 | 36.5/6.65 | −4.9* | −3.6 | −1.3* | 0.006 |
| **3308** | enolase 3, **fgm** | gil113205498 | 117 | 39 | 14 | 47.1/8.05 | 38.3/6.33 | −1.6* | −1.1 | −1.5* | 0.004 |
| **6203** | enolase 3, **fgm** | gil113205498 | 77 | 20 | 9 | 47.1/8.05 | 32.6/6.72 | −2.5* | −1.1 | −2.2* | 0.001 |
| **5203** | enolase 3, **fgm** | gil122134154 | 73 | 39 | 14 | 47.1/8.05 | 33.0/6.58 | −2.3* | 1.0 | −2.3* | 0.004 |
| 4309 | enolase 3, **fgm** | gil113205498 | 160 | 41 | 20 | 47.1/8.05 | 38.3/6.51 | | | | NS |
| 6410 | pyruvate kinase 3 isoform 1 **fgm** | gil194038728 | 86 | 31 | 13 | 57.8/7.96 | 38.4/6.67 | | | | NS |
| **1311** | phosphoglycerate kinase 1 **fgm** | gil47169449 | 77 | 23 | 10 | 44.4/8.01 | 38.6/5.89 | −2.6* | −1.5 | −1.7* | 0.001 |
| **4007** | albumin **fgm** | gil833798 | 66 | 16 | 9 | 69.3/5.92 | 19.4/6.51 | −7.4* | −4.6 | −1.6* | 0.015 |
| **1511** | albumin, **fgm** | gil833798 | 105 | 31 | 17 | 69.3/5.92 | 52.7/5.88 | −2.0* | −1.3 | −1.5* | 0.004 |
| **1710** | heat shock cognate 71 kDa protein | gil55733108 | 84 | 14 | 7 | 70.7/5.33 | 71.2/5.62 | −2.5* | −1.3 | −1.9 | 0.039 |
| **0125** | ubiquitin carboxyl-terminal esterase L1 | gil47523318 | 81 | 44 | 9 | 24.8/5.22 | 28.2/5.34 | −2.5* | 1.0 | −2.6* | 0.003 |
| 3811 | glycyl-tRNA synthetase | gil147902079 | 76 | 14 | 9 | 83/6.94 | 80.2/6.36 | | | | NS |
| **1213** | annexin IV | gil4033507 | 207 | 58 | 23 | 35.8/5.71 | 34.8/5.74 | −7.9* | −3.4 | −2.3* | 0.005 |
| **1716** | phosphoglucomutase-1 | gil122132319 | 135 | 35 | 17 | 61.5/6.36 | 64.9/5.78 | −2.2* | −1.2 | −1.8* | 0.0001 |
| 2707 | phosphoglucomutase-1 | gil122132319 | 101 | 21 | 10 | 61.5/6.36 | 64.4/5.97 | | | | NS |
| **3105** | triosephosphate isomerase 1 | gil90200404 | 138 | 73 | 14 | 26.6/6.54 | 28.5/6.36 | −2.1 | −1.7 | −1.2* | 0.014 |
| **3207** | glycerol-3-phosphate dehydrogenase [NAD9$^+$] | gil149714300 | 102 | 33 | 14 | 37.5/6.08 | 33.7/6.36 | −2.0* | −1.3 | −1.5* | 0.001 |

[a] Protein name and accession numbers were derived from NCBI database. [b] The MASCOT baseline significant score is 66. [c] Percent of coverage of the entire amino acid sequence. [d] Number of matched peptides in the database search. [e] MW and p*I*, theoretical (recorded in NCBI database) and observed (calculated from the spot position on the gel). [f] Relative abundance: greatest average quantity/lowest average quantity. A minus sign in comparisons of NN and nn, NN and Nn, and Nn and nn indicates that the relative abundance of the protein is higher in NN (homozygous normal), Nn (heterozygous), and nn (homozygous mutant) groups, respectively. [g] *p* value from the ANOVA analysis of genotype effect (spot numbers in bold are significantly influenced by genotype). [i] Asterisk indicates difference according to the Bonferroni pairwise comparison between genotypes at the 5% significance level. [j] **fgm**, protein fragment.

to post-translational modifications. Thus, we identified three Hsp27 electrophoretic variants (**Table 3**). Western blots performed on 2-DE gels confirmed these identifications and showed two additional electrophoretic variants (**Figure 3A**). The MS spectrum of the most acid form of Hsp27 protein (spot 1101) further analyzed for post-translational modifications clearly indicated two probable phosphorylation sites (**Table 3**). Similarly, we identified three $\alpha\beta$-C electrophoretic variants (**Table 3**). Western blots performed on 2-DE gels confirmed these identifications and showed two additional spots (**Figure 3A**). Finally, of the two heat-shock cognate (Hsc71) electrophoretic variants (**Table 4**), only one was more abundant in the NN. Western blots performed on 2-DE gels (**Figure 3A**) confirmed these identifications and showed four additional Hsc71 spots. The 1-DE Western blots (**Figure 3B**) performed on these three chaperone proteins showed that total amounts of the different isoforms of Hsp27 (nn, $0.64 \pm 0.42$; NN, $1.72 \pm 0.72$; $p = 0.007$) and of $\alpha\beta$-C (nn, $0.68 \pm 0.39$; NN, $2.2 \pm 1.1$; $p = 0.007$) were more abundant in the soluble fraction of NN compared to the nn genotype ($p = 0.007$). Total amounts of the different isoforms of Hsc71 (nn, $1.15 \pm 0.3$; NN, $0.62 \pm 0.23$) of the soluble fraction, did not differ between genotypes ($p = 0.06$). The antibodies used were specific for each of the proteins tested, as no cross-reactions were observed on the 1-DE Western blots.

$pH_{45(LL)}$ and Bradford values were correlated with 72 and 49 spots, respectively, which is more than expected by chance at the 5% level (binomial test $p < 0.001$). The other phenotypic variables were correlated with 2−20 spots, that is, not more than expected by chance (binomial test $p > 0.12$). Forty-one of the correlations with $pH_{45(LL)}$ were positive (Pearson *r* ranging from 0.49 to 0.82). Identified spots involve Hsp27, $\alpha\beta$-C, myofibrillar proteins (myosin light chain, actin) and AMPK. Negative correlations (Pearson *r* ranging from −0.49 to −0.81) were found with four enolase spots, a creatine kinase fragment, an Hsc71, and a myoglobin isoform. $pH_{45(LL)}$ and correlated spots were introduced into a principal component analysis to produce a biplot illustrating relationships between protein content, $pH_{45(LL)}$, and genotype (**Figure 4**). For spots related simultaneously to $pH_{45(LL)}$ and genotype, $pH_{45(LL)}$ was introduced as covariate in the ANOVA. This generally produced nonsignificant models (both pH and genotype effects were nonsignificant), suggesting that effects of genotype and pH were confounded.

Higher Bradford values were associated with higher levels of ATP-synthetase, various structural/contractile proteins (myosin light chain, actin), and proteins involved in their maintenance (tubulin, cofilin, T-complex protein). Nineteen of the correlations with Bradford values were negative. Identified spots involve four creatine kinase fragments and five spots related to the glycolytic pathway (two enolase fragments, two phosphoglucomutase isoforms, glycerol-3-phosphate, and triosephosphate dehydrogenase). Inclusion of Bradford values as covariate in the ANOVA did not remove genotype effects. Bradford values and $pH_{45(LL)}$ were not correlated ($p = 0.23$).

## DISCUSSION

**pH Decline.** Our results corroborate previous studies showing that the RyR1 mutation increases the rate of early post-mortem pH fall (*19*, *20*). The lower value of $pH_{45}$ in the nn pigs of the present study suggests an increased metabolic response to slaughter stress, causing a faster pH decline, compared to the other genotypes. Although $pH_{45}$ was recorded here in the LL muscle only, it is likely that other muscles, including the SM, showed also an increased rate of pH fall in nn pigs. Post-mortem pH evolution shows often the same tendencies in different muscles within an

**Table 6.** Pig Semimembranosus Muscle Proteins Differentially Expressed between Genetic Groups (Not Included in a Cluster)

| | | | | | | $M_w$ (kDa)/p*I* | | relative abundance [f] | | | |
|---|---|---|---|---|---|---|---|---|---|---|---|
| spot | protein name [a] | accession no. [a] | mowse score [b] | sequence coverage [c] | MP [d] | theor [e] | obsd [e] | NN vs nn | NN vs Nn | Nn vs nn | spot *p* value [g] |
| | | | Spots More Abundant in NN Genotype | | | | | | | | |
| **0012** | myosin regulatory light chain 2 | gil54607195 | 76 | 60 | 9 | 18.9/4.9 | 19.4/5.05 | 9.6*[h] | 3.7 | 2.5 | 0.001 |
| **1304** | pyruvate dehydrogenase: subunit = $\beta$ | gil448581 | 120 | 55 | 20 | 35.7/5.38 | 35.6/5.57 | 1.6* | 1.3 | 1.1 | 0.029 |
| **1502** | similar to ubiquinol-cytochrome *c* reductase | gil194041191 | 178 | 51 | 24 | 52.6/5.76 | 49.2/5.42 | 2.1* | −1.1 | 2.3* | 0.006 |
| **1803** | ubiquinone oxidoreductase | gil47117271 | 102 | 21 | 18 | 79.6/5.51 | 80.1/5.48 | 1.5 | −1.2 | 1.9* | 0.042 |
| **4701** | phosphoglucomutase-1 | gil122132319 | 191 | 41 | 23 | 61.5/6.36 | 67.3/6.42 | 1.2 | −1.0 | 1.2* | 0.033 |
| **5806** | WD repeat protein 1, isoform 10 | gil114593195 | 79 | 34 | 14 | 66.1/6.21 | 73.6/6.6 | 1.4 | −1.3 | 1.9* | 0.006 |
| **5801** | WD repeat protein 1 | gil12643636 | 157 | 35 | 19 | 66.1/6.17 | 73.3/6.54 | 1.2 | −1.1 | 1.3* | 0.017 |
| **0122** | $\rho$ GDP-dissociation inhibitor 1 | gil121107 | 84 | 48 | 10 | 23.4/5.12 | 28.5/4.97 | 2.1* | 1.7 | 1.2 | 0.048 |
| **2502** | $\gamma$-aminobutyraldehyde dehydrogenase | gil1049219 | 68 | 17 | 7 | 53.4/6.01 | 53.0/5.97 | 1.2* | −1.0 | 1.3* | 0.002 |
| **1208** | glutathione *S*-transferase $\mu$ 2 | gil118403788 | 90 | 43 | 13 | 25.7/6.9 | 30.1 5.7 | 3.4* | 1.4 | 2.4* | 0.003 |
| **1214** | non-selenium glutathione phospholipid hydroperoxide peroxidase | gil6689393 | 85 | 40 | 9 | 25/5.73 | 29.6/5.54 | 2.1 | 2.1* | −1.0 | 0.005 |
| | | | Spots More Abundant in nn Genotype | | | | | | | | |
| **3204** | glycogen phosphorylase **fgm**[i] | gil1364243 | 79 | 40 | 13 | 30.8/7.14 | 31.7/6.31 | −1.8* | 1.0 | −1.9 | 0.017 |
| **3010** | chain B, wild type deoxymyoglobin | gil3660247 | 83 | 54 | 7 | 16.9/6.83 | 18.3/6.19 | −18.6* | 1.1 | −19.8* | 0.002 |
| **5805** | transferrin | gil833800 | 143 | 35 | 21 | 76.9/6.73 | 82.6/6.57 | −1.6* | 1.0 | −1.6 | 0.023 |
| **2108** | Parkinson's disease protein 7 (DJ-1) | gil118403904 | 118 | 68 | 12 | 19.9/6.33 | 26.4/5.96 | −1.1 | 1.2 | −1.3* | 0.044 |

[a] Protein name and accession numbers were derived from NCBI database. [b] The MASCOT baseline significant score is 66. [c] Percent of coverage of the entire amino acid sequence. [d] Number of matched peptides in the database search. [e] MW and p*I*, theoretical (recorded in NCBI database) and observed (calculated from the spot position on the gel). [f] Relative abundance: greatest average quantity/lowest average quantity. A minus sign in comparisons of NN and nn, NN and Nn, and Nn and nn indicates that the relative abundance of the protein is higher in NN (homozygous normal), Nn (heterozygous), and nn (homozygous mutant) groups, respectively. [g] *p* value from the ANOVA analysis of genotype effect (spot numbers in bold are significantly influenced by genotype). [h] Asterisk indicates difference according to the Bonferroni pairwise comparison between genotypes at the 5% significance level. [i] **fgm**, protein fragment.

individual animal (*3*, *21*). Whereas proteomic profiles of muscles of different energetic metabolism types show large differences in glycolytic enzymes abundance (*14*, *22*), the present results show that increased post-mortem glycolysis was associated only with higher abundance of triose phosphate isomerase, which catalyzes the reversible interconversion of dihydroxyacetone phosphate and glyceraldehyde-3-phosphate. One phosphoglucomutase isoform was increased in nn pigs, another in NN pigs. This is in accordance with the review of Scheffler and Gerrard, suggesting there is no evidence supporting that PSE condition or faster post-mortem pH decline might be causally related to increased levels of energy metabolism related enzymes (*23*). On the basis of various studies, the authors indicate that levels or activities of the rate-limiting enzymes of glycogenolysis and glycolysis are often not different between normal and PSE muscles and, in any case, not correlated with early post-mortem pH decline. They suggest that other glycogenolysis modulating mechanisms contribute to altered post-mortem glycolysis, for example, AMPK. This protein is a cellular energy sensor, activated by high AMP/ATP and Cr/PCr ratios and low intracellular pH (*24*, *25*). Once activated, AMPK activates phosphorylase kinase, which in turn activates glycogen phosphorylase and promotes glycogenolysis. The present results show that the two identified isoforms of the regulatory subunit of AMPK were less abundant in nn genotype and associated with higher pH, suggesting that the identified isoforms are the inactive AMPK forms. Alternatively, and maybe more likely, nn muscles have lower AMPK levels as an adaptation of the cell to fluctuations in ATP levels resulting from varying intracellular $Ca^{2+}$ levels.

**Aerobic ATP Synthesis.** Proteins involved in aerobic ATP synthesis were less abundant in nn muscles. These proteins involve pyruvate dehydrogenase, which transforms pyruvate (output of the aerobic glycolysis) to acetyl CoA, used in the citric acid cycle, and various mitochondrial proteins: enzymes of the citric acid cycle (succinyl-CoA ligase and dihydropilamide succinyltransferase) and elements of the electron transport chain involved in oxidative phosphorylation (the ubiquinol cytochrome *c* reductase, the ubiquinone oxidoreductase, and the mitochondrial ATP synthase). The lower quantity of proteins involved in aerobic ATP resynthesis may reflect a decrease of mitochondrial volume or density in nn pigs, either of which would result in a lower capacity to synthesize mitochondrial ATP. This is in accordance with previous reports. Marple and Cassens reported that HAL-sensitive pigs (nn) exhibit a proportionally greater mass of white anaerobic fibers, lower oxidative capacity, and a lower capacity to produce ATP by oxidative phosphorylation (*26*). In addition, Eikelenboom and Van den Berg measured lower oxygen consumption in the mitochondria of nn pigs (*27*).

**Mitochondrial Oxidative Phosphorylation and Oxidative Stress.** Mitochondrial oxidative phosphorylation allows the reduction of $O_2$ to $H_2O$ while maximizing ATP synthesis. It produces both reactive oxygen species (ROS) and nitric oxygen species (NOS), which may function at low levels as signaling molecules in the regulation of fundamental cell activities, but which at higher levels are damaging byproducts. The potentially negative side-effects of ROS and NOS are counteracted by antioxidant defense systems. In the present study, antioxidant proteins were less abundant in nn muscles, which is coherent with the supposed lower ROS and NOS production. These proteins involve five proteins of the aldehyde dehydrogenase family, required for the clearance of potentially toxic aldehydes derived from lipid oxidation; glutathione peroxidase, a powerful antioxidant; and glutathione transferase, catalyzing the conjugation of a large number of hydrophobic electrophiles to glutathione.

**Chaperone-Related Proteins.** Cluster analysis indicated further that nn muscles were characterized by lower quantities of various spots identified as chaperone or chaperone-related proteins (Hsp27, $\alpha\beta$-C, Hsc71, and Hsc70/Hsp90). These proteins are

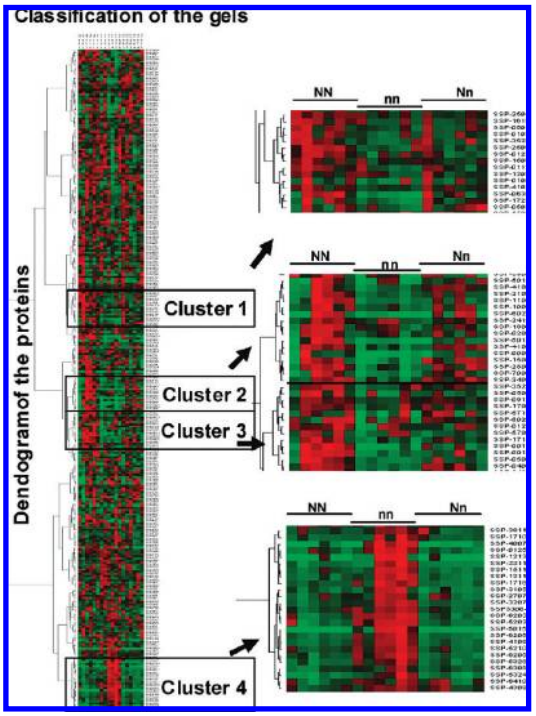


**Figure 1.** Heat map representation of the one-way hierarchical clustering analysis (processed with PermutMatrix according to the Pearson distance and Ward's aggregation method) after a log-ratio transformation of averaged detected and matched spot quantities. Numerical values from the data set were converted into a gradation of colors: red for high value and green for low value. The classification of the columns corresponding to the gels was constrained according to genotype. The rows corresponding to detected and matched spot intensities were automatically permuted in such a way that a statistical organization in the data set was revealed. The dendogram of spots allows four clusters of coregulated proteins to be distinguished according to genotype.

involved in refolding damaged proteins, maintenance of structural proteins, prevention of protein aggregation, and the redirection of unrepaired proteins to the proteolytic system. They have further crucial roles in muscle functioning. For example, Hsc71 is implicated in the folding and assembly pathways of myosin (*28*, *29*). Hsp27 associates with tropomyosin and actin during smooth muscle contraction (*30*, *31*). Small Hsp's form large homo- or hetero-oligomers (*32*, *33*). The oligomeric state and Hsp's activities are regulated by phosphorylation, which is consistent with the presence of different electrophoretic variants of the Hsp's found in the present study (*34*, *35*). Phosphorylation of Hsp27 is rapidly induced by reactive oxygen metabolites and other forms of stress and essential for its protective function at the level of actin filaments (*31*, *34*, *36*). Stress results further, within hours, in increased *Hsp* expression. In skeletal muscle, Hsc71 and Hsp27 levels increase 48 h following a single resistance exercise bout, but only Hsc71 levels increase after nondamaging exercise (*37*−*39*). Neufer and Benjamin showed that longer term stimulation of the motor nerve increased αβ-C and Hsp27 expression at RNA and protein levels (*40*).

**Chaperone Proteins and Meat Quality.** Various studies found relationships between intensities of Hsp's spots, *Hsp* expression, and meat characteristics, but these relationships vary. In accordance with the present results, lower abundance of Hsp27 and αβ-C was associated with the development of PSE zones in the SM and lighter color of pork meat, often indicative of a relatively low early post-mortem pH (*10*, *41*). Another study on pork found, however, that *Hsp72* expression and early post-mortem pH decline were negatively correlated (*71*). Studies on beef found also contrasting results. Increased Hsp27 in the early post-mortem period predicted increased tenderness 14 days later (*42*). In another study, higher Hsp27 levels were found in beef that was darker, less red, and less tender, containing less intramuscular fat, compared to their counterparts (*43*). Negative correlations were also found between *Hsp40* expression and tenderness (*44*). Contrasting results were further found in studies on total and sarcoplasmic protein fractions of pig or rat muscle showing that increased Hsp27 levels may be associated with higher or lower levels of enzymes of the glycolytic pathway (*14*, *22*, *41*, *45*, *46*).

**Protein Solubility.** The lower Hsp levels in nn muscles of the present study may be indicative of lower *Hsp* expression levels in nn muscles, but this seems to contrast with their generally faster metabolism. Alternatively, lower Hsp levels may be related to a lower extractability of these proteins in nn muscles. A recent study found that with increasing muscle acidity, small Hsp's including Hsp27 and αβ-C disappeared from the soluble muscle extracts and appeared in the insoluble fraction (*47*). In accordance with this, Kwasiborski et al. observed lower abundance of small Hsp's in extracts of early post-mortem muscle characterized by increased metabolic activity (*22*). Lower Hsp levels in nn muscle extracts may thus reflect reduced solubility of these proteins. One mechanism may be isoelectric precipitation, which occurs when the environmental pH approaches the isoelectric point of the protein, around 6 for certain Hsp27 isoforms (*47*). Alternatively, or in addition, due to the higher metabolic activity of nn muscles, Hsp's may be actively recruited by myofibrillar or denatured proteins (*47*) or trapped in the acto-myosin complex (*22*). The acto-myosin bonding might be stronger or more extensive in nn muscles, earlier characterized by an increased number of cells containing supercontracted myofibrils (*48*). The present results show accordingly that myofibril extractability was reduced in nn muscles and associated with lower abundance not only of Hsp's but of several other proteins known to associate with myofibrils. These involve (cluster 3) cofilin-2, involved in the regulation of actin, and translationally controlled tumor protein and T-complex protein, both involved in the assembly and disassembly of actin and tubulin. WD-repeat protein, involved in actin polymerization, and ρ GDP-dissociation inhibitor 1, involved in the disassembly of actin filaments, showed also lower levels in nn muscle extracts. Earlier studies found also lower extractability of proteins, including glycolytic enzymes and myofibrillar proteins, in PSE compared to normal meat (*49*−*52*). In the present study, total amounts of extracted proteins did not differ between genotypes, suggesting that the contribution of myofibrillar and associated proteins to the total soluble protein content was relatively small at the time of sampling.

**Protein Solubility and Proteolysis.** Various studies report a lower degree of myofibrillar protein degradation during post-mortem aging in PSE meat and increased myofibrillar resistance to compression, suggesting decreased proteolysis (*19*, *49*, *54*, *55*). Reduced proteolysis in nn muscles is partly explained by reduced endogenous proteolytic action, due to increased early post-mortem muscle temperature (*56*−*60*) or lower early post-mortem pH (*61*). It was further suggested that accessibility of myofibrils to endogenous proteolytic action may be reduced in PSE meat (*51*). The present results suggest that these phenomena could be related to increased acto-myosin bonding, as well as to increased protein aggregation and coprecipitation due to the increased abundance of fragments of glycolytic enzymes in nn muscles. Such increased fragmentation in nn muscles is well-known and believed to result from the combined effects of low early post-mortem pH values while muscle temperature is

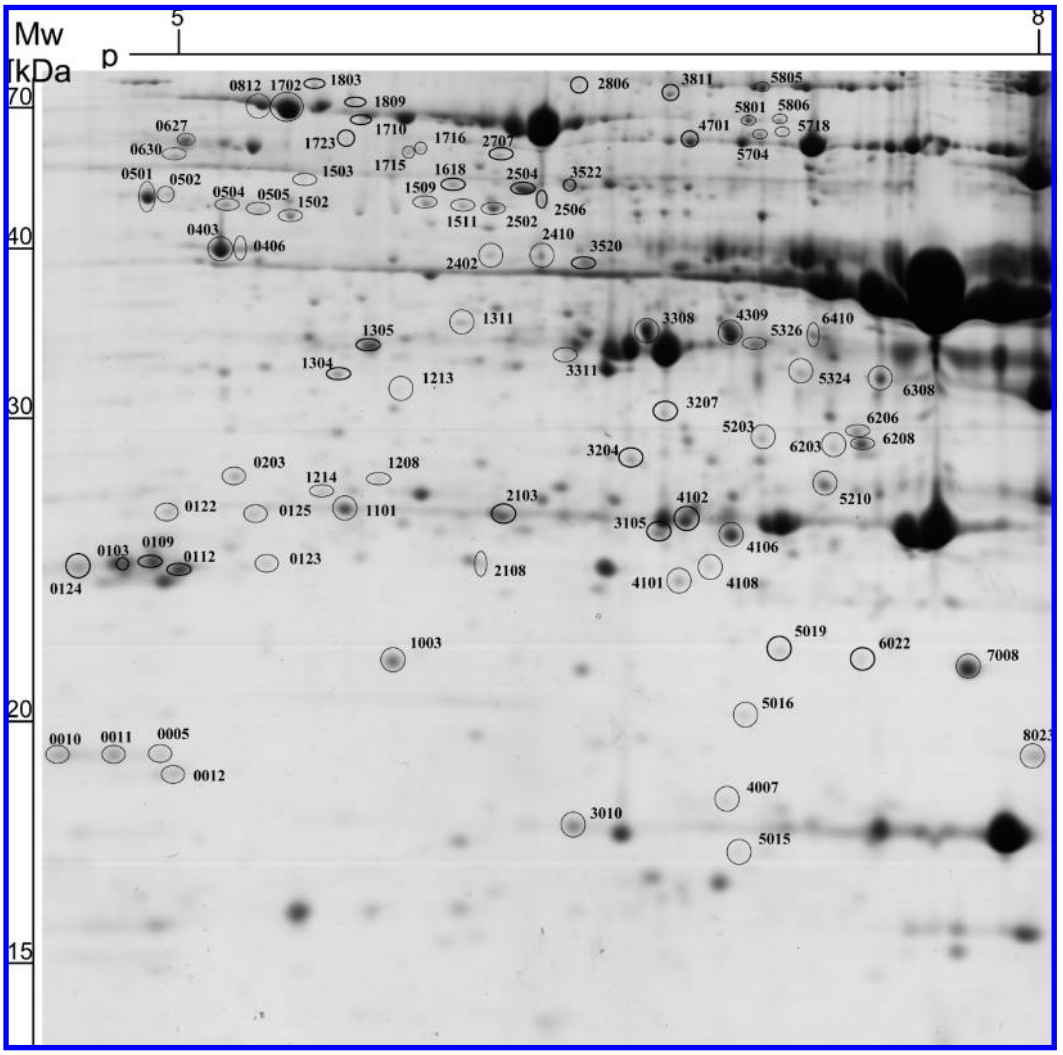


**Figure 2.** Representative 2-DE gel map of muscle sarcoplasmic proteins. The differentially expressed proteins between genotypes and the coregulated proteins evidenced by HCA are encircled and designated by their identification number. Correspondence between identification number and protein name is given in **Tables 2**−**6**.

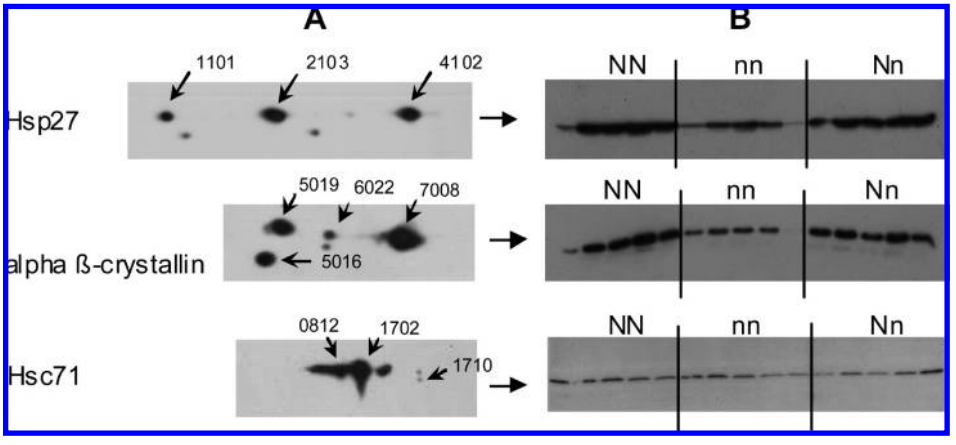


**Figure 3.** (**A**) Western blotting of Hsp27, α*β*-crystallin, and Hsc71 in a representative 2-DE gel, showing electrophoretic variants of each protein. (**B**) Western blotting of Hsp27, α*β*-crystallin, and Hsc71 in 1-DE gel of the soluble fraction, showing relative abundance of proteins between genotypes (NN, homozygous normal; nn, homozygous for the mutation, Nn, heterozygous).

still high (*62*). Our results suggest that increased protein fragmentation may further be due to the lower antioxidant protection and repair capacities of the nn muscle cells. Various studies suggest that Hsp's could play a role in tenderization during aging, but the exact mechanisms remain to be elucidated (*42*, *44*, *63*). The above studies and the present results suggest that cellular responses to stress may be central to reduced tenderization.

In addition to glycolytic fragments, a few full-length proteins were more abundant in the nn genotype. Annexin IV binds phospholipids in a $Ca^{2+}$-dependent manner and regulates the intracellular $Ca^{2+}$ signal (*64*). Its higher abundance may be

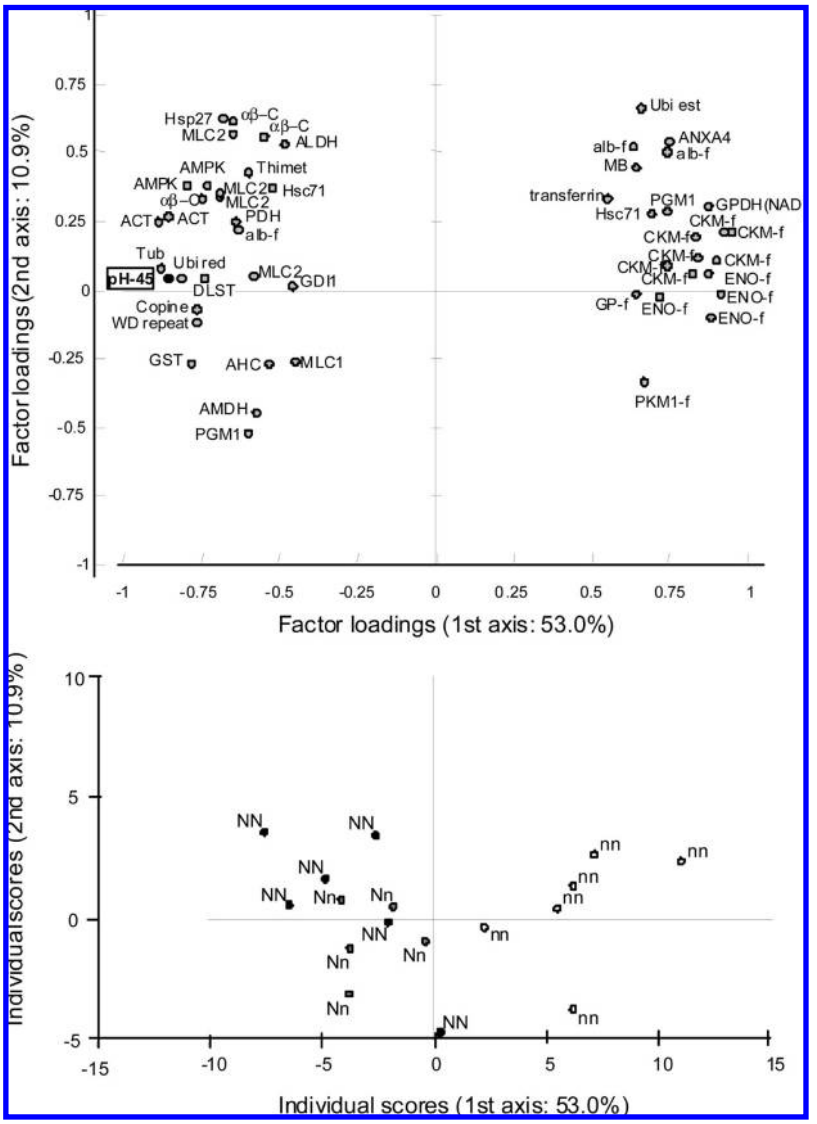


**Figure 4.** Principal component analysis biplot (first two principal axes) carried out on $pH_{45(LL)}$ (black dot) and all correlated spots (gray dots), showing factor loadings of all variables (top) and individual scores of pigs according to their genotype NN, Nn, or nn (bottom). ACT, actin; AHC, *S*-adenosylhomocysteinase; Alb-f, albumin fragment; ALDH, aldehyde dehydrogenase family; $\alpha\beta$-C, $\alpha$ $\beta$-crystallin; AMDH, $\gamma$-aminobutyraldehyde dehydrogenase; AMPK, cAMP-dependent protein kinase; ANXA4, annexin 4; CKM-f, creatine kinase, muscle, fragment; DLST, dihydrolipoamide *S*-succinyltransferase; ENO-f, enolase fragment; GDI1, $\rho$ GDP-dissociation inhibitor 1; GP-f, glycogen phosphorylase fragment; GPDH(NAD), glycerol-3-phosphate dehydrogenase [$NAD^+$]; GST, glutathione *S*-transferase $\mu$; Hsc71, heat shock cognate 71 kDa; Hsp27, heat shock protein 27 kDa; MB, myoglobin; MLC1, myosin light chain isoform 1; MLC2, myosin light chain isoform 2; PDH, pyruvate dehydrogenase, $\beta$-subunit; PGM1, phosphoglucomutase-1; PKM1-f, pyruvate kinase 3 isoform 1 fragment; Thimet, thimet oligopeptidase; Tub, tubulin, $\alpha$ 4a; Ubi est, ubiquitin carboxyl-terminal esterase L1; Ubi red, similar to ubiquinol-cytochrome-*c* reductase; WD repeat, WD repeat protein 1.

related to the deficiency in $Ca^{2+}$ regulation in nn muscles. Transferrin is an indicator of hypoxic status of the muscle (*65*) and might be related to the reduced capillary network observed in nn muscles, possibly resulting in a chronic hypoxic state (*14*, *66*, *67*). Finally, one spot (3010) of myoglobin was 18.6 times more abundant in the nn genotype. Its higher abundance may serve to counteract the possibly reduced $O_2$ tension or to regulate bioactive ROS, NOS, and lipid radicals, another function of myoglobin (*68*−*70*).

In conclusion, results give further insight into the relationship between protein denaturation, aggregation, and precipitation and the development of the PSE meat quality defect (*8*, *9*). Summarizing, 18% of the proteins were influenced by the nn genotype and another 10% were coregulated with these influenced proteins, as indicated by cluster analysis. Results suggest that compared to NN and/or Nn muscles, nn muscles are less oxidative and have less antioxidative and repair capacities. Results show further that the faster early post-mortem pH decline was not associated with the increased presence of glycolytic enzymes in nn muscles, but could explain at least part of the lower extractability of myofibrillar and associated proteins. The faster pH decline and reduced antioxidant and repair capacities may have contributed to the increased protein fragmentation observed in nn muscles. Hypercontraction of myofibrillar proteins, protein aggregation, and precipitation on myofibrils may reduce their exposure to endogenous proteolytic action and contribute to the reduced tenderization process observed in PSE meat.

Results suggest protein mechanisms underlying the effect of cellular stress responses on meat quality, including the nn condition, and point to a central role of cell adaptative states counteracting protein denaturation. Additional studies are needed to determine if proteins of the cellular protective system can be used as markers for

meat quality traits or as genetic selection criteria. Further studies are needed to elucidate the role of cellular stress responses during the preslaughter period in normal, non-HAL n carrier pigs.

## LITERATURE CITED


(1) Fujii, J.; Otsu, K.; Zorzato, F.; De Leon, S.; Khanna, V. K.; Weiler, J.; O'Brien, P. J.; Maclennan, D. H. Identification of a mutation in the porcine ryanodine-receptor that is associated with malignant hyperthermia. *Science* **1991**, *253*, 448–451.

(2) Michelson, J.; Gallant, E.; Litterer, L.; Johnson, K.; Rempel, W.; Louis, C. Abnormal sarcoplasmic reticulum ryanodine receptor in malignant hyperthermia. *J. Biol. Chem*. **1988**, *263*, 9310–9315.

(3) Terlouw, E. M. C.; Rybarczyk, P. Explaining and predicting differences in meat quality trough stress reactions at slaughter: the case of Large White and Duroc pigs. *Meat Sci*. **2008**, *79*, 795–805.

(4) Sybesma, W.; Eikelenboom, G. Malignant hyperthermia syndrome in pigs. *Neth. J. Vet. Sci*. **1969**, *2*, 155–160.

(5) Gallant, E. M.; Lentz, L. R. Excitation−contraction coupling in pigs heterozygous for malignant hyperthermia. *Am. J. Physiol*. **1992**, *262*, C422–426.

(6) Sellier, P.; Monin, G. Genetics of pig meat quality: a review. *J. Muscle Foods* **1994**, *5* (2), 187–219.

(7) Sellier, P. Genetics of meat and carcass traits. In *The Genetics of the Pig*; Rothschild, M. F., Ruvinsky, A., Eds.; CAB International: Oxon, U.K., 1998; pp 463−510.

(8) Bendall, J. R.; Wismer-Peterson, J. Some properties of the fibrillar proteins of normal and watery pork muscle. *J. Food Sci*. **1962**, *27*, 144–157.

(9) Joo, S. T.; Kauffman, R. G.; Kim, B. C.; Park, G. B. The relationship of sarcoplasmic and myofibrillar protein solubility to colour and water-holding capacity in porcine longissimus muscle. *Meat Sci*. **1999**, *52*, 291–297.

(10) Laville, E.; Sayd, T.; Santé-Lhoutellier, V.; Morzel, M.; Labas, R.; Franck, M.; Chambon, C.; Monin, G. Characterisation of PSE zones in *semimembranosus* pig muscle. *Meat Sci*. **2005**, *70*, 167–172.

(11) Barbut, S.; Sosnicki, A. A.; Lonergan, S. M.; Knapp, T.; Ciobanu, D. C.; Catcliffe, L. J.; Huff-Lonergan, E.; Wilson, E. W. Progress in reducing the pale, soft and exudative (PSE) problem in pork and poultry meat. *Meat Sci*. **2008**, *79*, 46–63.

(12) Otsu, K.; Phillips, M. S.; Khanna, V. K.; de Leon, S.; MacLennan, D. H. Refinement of diagnostic assays for a probable causal mutation for porcine and human hyperthermia. *Genomics* **1992**, *13*, 835–837.

(13) Laville, E.; Sayd, T.; Terlouw, C.; Chambon, C.; Damon, M.; Larzul, C.; Leroy, P.; Glenisson, G.; Chérel, P. Comparison of sarcoplasmic proteomes between two groups of pig muscles selected for shear force of cooked meat. *J. Agric. Food Chem*. **2007**, *55*, 5834–5841.

(14) Hamelin, M.; Sayd, T.; Chambon, C.; Bouix, J.; Bibé, B.; Milenkovic, D.; Leveziel, H.; Georges, M.; Clop, A.; Marinova, P.; Laville, E. Proteomic analysis of the ovine "Belgian Texel" breed muscle hypertrophy. *J. Anim. Sci*. **2006**, *84*, 3266–3276.

(15) Morzel, M.; Chambon, C.; Lefèvre, F.; Paboeuf, G.; Laville, E. Modification of trout (*Oncorhynchus mykiss*) by preslaughter activity. *J. Agric. Food Chem*. **2006**, *54*, 2997–3001.

(16) Meunier, B.; Bouley, J.; Piec, I.; Bernard, C.; Picard, B.; Hocquette, J. F. Data analysis methods for detection of differential protein expression in two-dimensional gel electrophoresis. *Anal. Biochem*. **2005**, *340*, 226–230.

(17) Caraux, G.; Pinloche, S. PermutMatrix: a graphical environment to arrange gene expression profiles in optimal linear order. *Bioinformatics* **2005**, *21*, 1280–1281.

(18) Meunier, B.; Dumas, E.; Piec, I.; Béchet, D.; Hébraud, M.; Hocquette, J. F. Assessment of hierachical clustering methodologies for proteomic data mining. *J. Protein Res*. **2007**, *6*, 358–366.

(19) Monin, G.; Larzul, C.; Le Roy, P.; Culioli, J.; Mourot, J.; Rousset-Akrim, S.; Talmant, A.; Touraille, C.; Sellier, P. Effect of the halothane genotype and slaughter weight on texture of pork. *J. Anim. Sci*. **1999**, *77*, 408–415.

(20) Fernandez, X.; Neyraud, E.; Astruc, T.; Sante, V. Effects of halothane genotype and pre-slaughter treatment on pig meat quality. Part 1. Post mortem metabolism, meat quality indicators and sensory traits of m. Longissimus lumborum. *Meat Sci*. **2002**, *62*, 429–437.

(21) Huff-Lonergan, E.; Baas, T. J.; Malek, M.; Dekkers, J. C.; Prusa, K.; Rothschild, M. F. Correlations among selected pork quality traits. *J. Anim. Sci*. **2002**, *80*, 617–627.

(22) Kwasiborski, A.; Sayd, T.; Chambon, C.; Santé-Lhoutellier, V.; Rocha, D.; Terlouw, C. Pig *Longissimus lumborum* proteome: Part I. Effects of genetic background, rearing environment and gender. *Meat Sci*. **2008**, *80*, 968–981.

(23) Scheffler, T. L.; Gerrard, D. E. Mechanisms controlling pork quality development: the biochemistry controlling postmortem energy metabolism. *Meat Sci*. **2007**, *77*, 7–16.

(24) Ponticos, M.; Lu, Q. L.; Jennifer, E.; Morgan, J. E.; Grahame Hardie, D. G.; Partridge, T. A.; Carling, D. Dual regulation of the AMP-activated protein kinase provides a novel mechanism for the control of creatine kinase in skeletal muscle. *EMBO J*. **1998**, *17*, 1688–1699.

(25) Shen, Q. W.; Means, W. J.; Underwood, K. R.; Thompson, S. A.; Zhu, M. J.; McCormick, R. J.; Ford, S. P.; Ellis, M.; Du, M. Early post-mortem AMP-activated protein kinase (AMPK) activation leads to phosphofructokinase-2 and -1 (PFK-2 and PFK-1) phosphorylation and the development of pale, soft and exudative (PSE) conditions in porcine longissimus muscle. *J. Agric. Food Chem*. **2006**, *54*, 5583–5589.

(26) Marple, D. N.; Cassens, R. G. A mechanism for stress-susceptibility in swine. *J. Anim. Sci*. **1973**, *37*, 546–550.

(27) Eikelenboom, G.; van den Bergh, S. G. Aberrant mitochondrial energy metabolism in stress-susceptible pigs. In *Proc. 2nd Int. Symp. Condition Meat Quality Pigs*; Pudoc: Wageningen, The Netherlands, 1971; p 66.

(28) Alberti, S.; Esser, C.; Höfeld, J. BAG-1 a nucleotide exchange factor of HCS70 with multiple cellular functions. *Cell Stress Chaperones* **2003**, *8*, 225–231.

(29) Srikakulam, R.; Winkelmann, D. A. Chaperone-mediated folding and assembly of myosin in striated muscle. *J. Cell Sci*. **2004**, *117*, 641–652.

(30) Schneider, G. B.; Hamano, H.; Cooper, L. F. In vivo evaluation of hsp27 as an inhibitor of actin polymerization: Hsp27 limits actin stress fiber and focal adhesion formation after heat shock. *J. Cell. Physiol*. **1998**, *177*, 575–584.

(31) Bitar, K. N. HSP27 phosphorylation and interaction with actin-myosin in smooth muscle contraction. *Am. J. Physiol. Gastrointest. Liver Physiol*. **2002**, *282*, G894–G903.

(32) Rogalla, T.; Ehrnsperger, M.; Preville, X.; Kotlyarov, A.; Lutsch, G.; Ducasse, C.; Paul, C.; Wieske, M.; Arrigo, A.-P.; Buchner, J.; Gaestel, M. Regulation of Hsp27 oligomerization, chaperone function, and protective activity against oxidative stress/tumor necrosis factor α by phosphorylation. *J. Biol. Chem*. **1999**, *274*, 18947–18956.

(33) Sugiyama, Y.; Suzuki, A.; Kishikawa, M.; Akutsu, R.; Hirose, T.; Waye, M. M. Y.; Tsui, S. K. W.; Yoshida, S.; Ohno, S. Muscle develops a specific form of small heat shock protein complex composed of MKBP/HSPB2 and HSPB3 during myogenic differentiation. *J. Biol. Chem*. **2000**, *275*, 1095–1104.

(34) Concannon, C. G.; Gorman, A. M.; Samali, A. On the role of Hsp27 in regulating apoptosis. *Apoptosis* **2003**, *8*, 61–70.

(35) Clemen, C. S.; Fischer, D.; Roth, U.; Simon, S.; Vicart, P.; Kato, K.; Kaminska, A. M.; Vorgerd, M.; Goldfarb, L. G.; Eymard, B.; Romero, N. B.; Goudeau, B.; Eggermann, T.; Zerres, K.; Noegel, A. A.; Schröder, R. Hsp27-2D-gel electrophoresis is a diagnostic tool to differentiate primary desminopahies from myofibrillar myopathies. *FEBS Lett*. **2005**, *579*, 3777–3782.

(36) Huot, J.; Lambert, H.; Lavoie, J. N.; Guimond, A.; Houle, F.; Landry, J. Characterization of 45-kDa/54-kDa HSP27 kinase, a stress-sensitive kinase which may activate the phosphorylation-dependent protective function of mammalian 27-kDa heat-shock protein HSP27. *Eur. J. Biochem*. **1995**, *227*, 416–427.

(37) Thompson, H. S.; Maynard, E. B.; Morales, E. R.; Scordilis, S. P. Exercise-induced HSP27, HSP70 and MAPK responses in human skeletal muscle. *Acta Physiol. Scand*. **2003**, *178*, 61–72.

(38) Morton, J. P.; MacLaren, P. M.; Cable, N. T.; Bongers, T.; Griffiths, R. D.; Campbell, I. T.; Evans, L.; Kayani, A.; McArdle, A.; Drust, B.

Time course and differential responses of the major heat shock protein families in human skeletal muscle following acute nondamaging treadmill exercise. *J. Appl. Physiol*. **2006**, *101*, 176–182.
(39) Folkesson, M.; Mackey, A. L.; Holm, L.; Kjaer, M.; Paulsen, G.; Raastad, T.; Henriksson, J.; Kadi, F. Immunohistochemical changes in the expression of HSP27 in exercised human vastus lateralis muscle. *Acta Physiol*. **2008**, *194*, 215–222.
(40) Neufer, P. D.; Benjamin, I. J. Differential expression of αB-crystallin and Hsp27 in skeletal muscle during continuous contractile activity. *J. Biol. Chem*. **1996**, *271*, 24089–24095.
(41) Sayd, T.; Morzel, M.; Chambon, C.; Franck, M.; Figwer, P.; Larzul, C.; Le Roy, P.; Monin, G.; Chérel, P.; Laville, E. Proteome analysis of the sarcoplasmic fraction of pig *semimembranosus* muscle: implications on meat colour development. *J. Agric. Food Chem*. **2006**, *54*, 2732–2737.
(42) Morzel, M.; Terlouw, C.; Chambon, C.; Micol, D.; Picard, B. Muscle proteome and meat eating qualities of *longissimus thoracis* of "Blonde d'Aquitaine" young bulls: a central role of HSP27 isoform. *Meat Sci*. **2008**, *78*, 297–304.
(43) Kim, N. K.; Cho, S.; Lee, S. H.; Park, H. R.; Lee, C. S.; Cho, Y. M.; Choy, Y. H.; Yoon, D.; Im, S. K.; Park, E. W. Proteins in *longissimus* muscle of Korean native cattle and their relationship to meat quality. *Meat Sci*. **2008**, *80*, 1068–1073.
(44) Bernard, C.; Cassar-Malek, I.; Le Clunff, M.; Dubroeucq, H.; Renand, G.; Hocquette, J. F. New indicators of beef sensory quality revealed by expression of specific genes. *J. Agric. Food Chem*. **2007**, *55*, 5229–5237.
(45) Lametsch, R.; Kristensen, L.; Larsen, M.; RTherkildsen, M.; Oksbjerg, N.; Ertbjerg, P. Changes in the muscle proteome after compensatory growth in pigs. *J. Anim. Sci*. **2006**, *84*, 918–924.
(46) Piec, I.; Listrat, A.; Alliot, J.; Chambon, C.; Taylor, R. G.; Bechet, D. Differential proteome analysis of aging in rat skeletal muscle. *FASEB J*. **2005**, *19*, 1143–1145.
(47) Pulford, D. J.; Fraga Vasquez, S.; Frost, D. F.; Fraser-Smith, E.; Dobbie, P.; Rosenvold, K. The intracellular distribution of small heat shock proteins in post-mortem beef is determined by ultimate pH. *Meat Sci*. **2008**, *79*, 623–630.
(48) Palmer, E. G.; Topel, D. G.; Christian, L. L. Microscopic observation of muscle from swine susceptible to malignant hyperthermia. *J. Anim. Sci*. **1977**, *45*, 1032–1035.
(49) Boles, J. A.; Parrish, F. C.; Huiatt, T. W.; Robson, R. M. Effect of porcine stress syndrome on the solubility and degradation of myofibrillar cytoskeletal proteins. *J. Anim. Sci*. **1992**, *70*, 454–464.
(50) Sather, A.; Jones, S. D. M. The effect of genotype on feedlot performance, carcass composition, and lean meat quality from commercial pigs. *Can. J. Anim. Sci*. **1996**, *76*, 507–516.
(51) Gil, M.; Hortós, M.; Sárraga, C. Calpain and cathepsin activities, and protein extractability during ageing of *longissimus* porcine muscle from normal and PSE meat. *Food Chem*. **1998**, *63*, 385–390.
(52) Channon, H. A.; Payne, A. M.; Warner, R. D. Halothane genotype, pre-slaughter handling and stunning method all influence pork quality. *Meat Sci*. **2000**, *56*, 291–299.
(53) Kang, C. G.; Nuguruma, M.; Fukazawa, T. Difference in Z line removal between normal and PSE porcine myofibrils. *J. Food Sci*. **1978**, *43*, 508–514.
(54) Minelli, G.; Culioli, J.; Vignon, X.; Monin, G. Postmortem changes in the mechanical properties and ultrastructure of the *longissimus* of two porcine breeds. *J. Muscle Foods* **1995**, *6*, 313–326.
(55) Fernandez, X.; Forslid, A.; Tornberg, E. The effect of high post-mortem temperature on the develoment of pale, soft and exudative pork: interaction with ultimate pH. *Meat Sci*. **1994**, *37*, 133–147.
(56) Dransfield, E. Optimisation of tenderisation, ageing and tenderness. *Meat Sci*. **1994**, *36*, 105–121.
(57) Koohmaraie, M. Biochemichal factors regulating the toughening and tenderization processes of meat. *Meat Sci*. **1996**, *43*, S191–S201.
(58) Hwang, I. H.; Thompson, J. M. The interaction between pH and temperature decline early post-mortem on the calpain system and objective tenderness in electrically stimulated beef *longissimus dorsi* muscle. *Meat Sci*. **2001**, *58*, 167–174.
(59) Rees, M. P.; Trout, G. R.; Warner, R. D. Tenderness of pork *m. longissimus thoracis et lumborum* after accelerated boning. Part I. Effect of temperature conditioning. *Meat Sci*. **2003**, *61*, 205–214.
(60) Hwang, I. H.; Park, B. Y.; Kim, J. H.; Cho, S. H.; Lee, J. M. Assessment of post-mortem proteolysis by gel-based analysis and its relationship to meat quality traits in pig *longissimus*. *Meat Sci*. **2005**, *69*, 79–91.
(61) Claeys, E.; De Smet, S.; Demeyer, D.; Geers, R.; Buys, N. Effect of rate of pH decline on muscle enzyme activities in two pig lines. *Meat Sci*. **2001**, *57*, 257–263.
(62) Offer, G. Modelling of the formation of pale, soft and exudative meat: effects of chilling regime and rate and extent of glycolysis. *Meat Sci*. **1991**, *30*, 157–184.
(63) Ouali, A.; Herrera-Mendes, C. H.; Coulis, G.; Becila, S.; Boudjellal, A.; Aubry, L. Revisiting the conversion of muscle into meat and the underlying mechanisms. *Meat Sci*. **2006**, *74* (1), 44–58.
(64) Kourie, J. I.; Wood, H. B. Biophysical and molecular properties of annexin-formed channels. *Prog. Biophys. Mol. Biol*. **2000**, *73*, 91–134.
(65) Lopez-Barneo, J.; Pardal, R.; Ortega-Saenz, P. Cellular mechanisms of oxygen sensing. *Annu. Rev. Physiol*. **2001**, *63*, 259–287.
(66) Essen-Gustavsson, B.; Karlson, A.; Lundström, K. Muscle fibre characteristics and metabolic response at slaughter in pigs of different halothane genotypes and their relation to meat quality. *Meat Sci*. **1992**, *31*, 1–11.
(67) Eu, J. P.; Sun, J.; Xu, L.; Stamler, J. S.; Meissner, G. The skeletal muscle calcium release channel: coupled $O_2$ sensor and NO signaling functions. *Cell* **2000**, *102*, 499–509.
(68) Brunori, M. Nitric oxide moves myoglobin centre stage. *TRENDS Biochem. Sci*. **2001**, *26*, 209–210.
(69) Lee, S.; Phillips, A. L.; Liebler, D. C.; Faustman, C. Porcine oxymyoglobin and lipid oxidation in vitro. *Meat Sci*. **2003**, *63*, 241–247.
(70) Gelfi, C.; De Palma, S.; Ripamonti, M.; Wait, R.; Eberini, I.; Bajracharya, A.; Marconi, C.; Schneider, A.; Hoppeler, H.; Cerretelli, P. New aspects of altitude adaptation in Tibetans. A proteomic approach. *FASEB J*. **2004**, *18*, 612–614.
(71) Kwasiborski, A.; Rocha, D.; Terlouw, C. Gene expression in Large White or Duroc-sired female and castrated male pigs, and relationships with pork quality. *Animal Genetics,* in press.

**Received January 26, 2009. Revised manuscript received April 3, 2009. This work was financially supported by grants from the Agence Nationale de la Recherche, Programme Alimentation-Nutrition Humaine (Decision ANR-06PNRA-025-05).**